Evaluation of Refractory Metal Concentrations in Nano-Particulate Pressed-Powder Pellets Using LA-ICP-MS

(article starts on next page)

minerals

MDPI

Article

Evaluation of Refractory Metal Concentrations in Nano-Particulate Pressed-Powder Pellets Using LA-ICP-MS

Lorena Guldris Leon [1,*], Johanne Lebrun Thauront [2], K. Johan Hogmalm [3], Erik Hulthén [1] and Johan Malmqvist [1]

[1] Department of Industrial and Materials Science, Chalmers University of Technology, 412 58 Gothenburg, Sweden; erik.hulthen@chalmers.se (E.H.); johan.malmqvist@chalmers.se (J.M.)

[2] Département de Chimie, École Normale Supérieure, PSL University, 75005 Paris, France; johanne.lebrun.thauront@ens.fr

[3] Department of Earth Sciences, University of Gothenburg, 413 20 Gothenburg, Sweden; johanh@gvc.gu.se

[*] Correspondence: lorena.guldris@chalmers.se; Tel.: +46-72-982-0250

Abstract: Whole-rock geochemical analysis is a standard method to measure the chemical composition of ores. Analysis of refractory ore metals such as Ta and W typically requires fused bead and acid digestion followed by inductively coupled plasma atomic emission spectrometry (ICP-AES) and inductively coupled mass spectrometry (ICP-MS). Since these techniques are time-consuming and expensive, there is a demand for methods that can quantitatively measure low elemental concentration of refractory ore metals using a less expensive and simple approach. This paper evaluates preparation and analytical procedures developed to obtain whole-rock element concentrations of ore samples and mineral concentrates. It shows that the production of nano-particulate pressed-powder pellets followed by LA-ICP-MS analysis of W and Ta ores can be used to determine, within the error margin, the concentrations of the refractory metals W, Ta, Nb, and Sn compared to a reference values obtained by solution analysis. The results have implications for developing a commercially viable method for analysis of refractory elements to benefit mineral processing given the simplicity and resource-efficiency of the combined pressed pellet production and laser ablation analytical methodology.

Keywords: LA-ICP-MS; trace elements; bulk sample analysis; nano-particulate pressed-powder tablets; tungsten; tantalum; critical metals; refractory metals

1. Introduction

In mineral processing, it is essential to obtain the chemical composition of the ore, including the concentrations of the major and minor rock-forming elements and trace elements, using analytical methods. Usually, the bulk chemical analysis is performed by fused bead and acid digestion of the samples, followed by inductively coupled plasma atomic emission spectrometry (ICP-AES) and inductively coupled plasma mass spectrometry (ICP-MS). The usage of ICP-AES and ICP-MS tests is a time-consuming and expensive process involving dissolution of refractory mineral phases [1].

It can be difficult to grind to a homogenous powder of some rock types that contain abundant refractory minerals. Refractory minerals such as zircon, alumina, corundum, garnet, or magnesia can survive the acid digestion as residual material, generating a low recovery for trace elements like tantalum, chromium, REE, and others [2–4].

Laser ablation inductively coupled plasma mass spectrometry (LA-ICP-MS) is currently applied in many research fields since it can determine trace element and isotope composition of minerals, rocks, ores, and sediments using direct solid sample analysis while avoiding pre-treatment such acid decomposition and contamination or loss of analytes during the preparation procedures [2,5–7]. Four major geological sample types are suitable for laser ablation analysis: synthesized minerals, homogeneous natural minerals, vitrified powders, and pressed-powder pellets [2]. However, from these four major geological

sample types, the pressed-powder pellets technique is the technique that has been reported as a strategy suitable for direct bulk analysis of solids by LA-ICP-MS, which can apply to all types of rock, minerals, and elements.

Gray, in 1985 [8], was one of the first researchers to develop a method using pressed-powder pellets manufactured for X-ray fluorescence (XRF). After him, other researchers tested and optimized the method without or with the addition of a binder [1]. The role of binders is to provide mechanical strength and cohesion to the pellet and increase the stability of the signal during the laser ablation, which results in stable and reproducible data. [9] The use of binders has been studied in several research papers and it has been established as helping to achieve the necessary mechanical strength and cohesion of the pellet as well as increasing the stability of the signal during the laser ablation, which results in stable and reproducible data [9]. Nano-particulate pressed-powder pellets (PPP) have previously been evaluated and studied in wet-milling protocols in aqueous suspension [2]. Of relevance to the previous study, the milling time, ball size, ball powder ratio, and water powder ratio were optimized until achieving particles sized lower than 1.5 μm for forming and analyzing PPP with good cohesion and homogeneity suitable for laser ablation. Peters and Pettke [10] enhanced the technique by comparing different types of binders and improving the acquisition of major elements.

Rock powders are a heterogeneous mixture of minerals with different chemical composition and physical properties [11]. To reduce the heterogeneity and increase the reproducibility of whole rock analysis of powder pellets, particle size needs to be reduced as much as possible, and samples must be homogenized so that all minerals occur in similar concentrations across all size fractions. Another factor of importance is the pelletizing pressure, representing the impact of the compactness of the sample. A closely packed sample produces measurements with higher intensity [12]. The use of binders has been recognized to increase pellets' mechanical strength and cohesion, achieving a more stable and reproducible signal during chemical analysis [10]. Graphite, cellulose, spectroBlend, and absorbing binders are the most commonly used binders.

Our study focuses on evaluating procedural protocols for preparing nano-particulate powder-pressed pellets that can be used to analyze refractory elements by LA-ICP-MS. We provide data on the chemical composition of refractory elements W, Ta, Nb, and Sn. Since ores containing the critical resource elements W and Ta have proven challenging to digest and homogenize for chemical analysis, the LA-ICP-MS method for bulk analysis of these elements has significance for refractory ores in general. Furthermore, the evaluation of sample preparation methods suitable for LA-ICP-MS analysis aid optimization of standard procedures for pellet production.

2. Materials

The application of the method was evaluated in well-known tungsten (W) and tantalum (Ta) ores. The Ta ore is a low-grade Sn–Ta greisen-type mineralization ore from the Penouta deposit located in Penouta village, in the municipality of Viana do Bola, Ourense, Galicia, in the northeast of Spain. The mineralization is hosted in leucogranite affected by greisen processes to the greisen and in the surrounding leucogranites. The Penouta leucogranite is hosted in metamorphic rocks, mainly constituted by gneisses and mica-schists [13,14]. The main valuable minerals are cassiterite (SnO_2) and columbite-group minerals, which constitute a solid solution with tantalite ((Fe,Mn) (Ta,Nb)$_2O_6$) and columbite ((Fe, Mn)(Nb, Ta)$_2O_6$) and four end members: columbite-(Fe), ($FeNb_2O_6$); columbite-(Mn), ($MnNb_2O_6$); tantalite-(Fe), ($FeTa_2O_6$); and tantalite-(Mn), ($MnTa_2O_6$) [15,16]. Other Ta-rich minerals, such as microlite and wodginite, have also been reported [13]. A detailed characterization of Penouta ore is described by Alfonso et al., 2018 [13]; Llorens González et al., 2017 [15], and López et al., 2018 [17].

The W ore is a scheelite ore of amphibolites and felsic gneisses from the polymetamorphic volcano-sedimentary Habach series from the Mittersill scheelite deposit located in Salzburg province, Austria [16]. The ore consisted of scheelite associated with calc-silicate

minerals. The Mittersill scheelite deposit represents metamorphosed W-bearing magmatic rocks [18,19]. Scheelite is exploited from veins hosted in an amphibolite rock mainly composed of quartz, plagioclase (albite), hornblende, actinolite, and K-feldspar, with biotite, muscovite, and epidote as minor minerals [18]. Mineable W concentrations (1% WO_3, max values up to 15% WO_3) occur exclusively in the hornblendite units and are hosted in concordant felsic gneisses and fabric-parallel as well as fabric-cross-cutting quartz veins. Major, trace, and rare earth-element data reveal that the ore-bearing hornblendite units are of boninitic parentage, suggesting that they formed from island-arc tholeiites [16,19].

3. Methods

The sample processing and measurement protocol used in this study is divided into five parts that are schematically illustrated in Figure 1. The first part relates to the sampling and reduction of the particles to achieve a size smaller than <75 μm. The second step in the process corresponds to the wet milling, where the particle size was reduced to nano sizes, involving a high-power planetary ball mill. The third part relates to the drying stage of the sample suspension. This step was performed and compared using four techniques to identify the influence of sample preparation parameters on the resulting samples' chemical distribution. The techniques used were freeze-dried (FD), evaporation (E), vacuum-driven sterile filter (VDSF), and vacuum-driven membrane filter (VDMF). The fourth step corresponds to the pellet pressing, produced both with and without a binder. The homogenization time between the binder and the ore powder was varied at 1 min, 5 min, and 10 min. The last part relates to the chemical characterization of the pellets through LA-ICP-MS and the evaluation of these results.
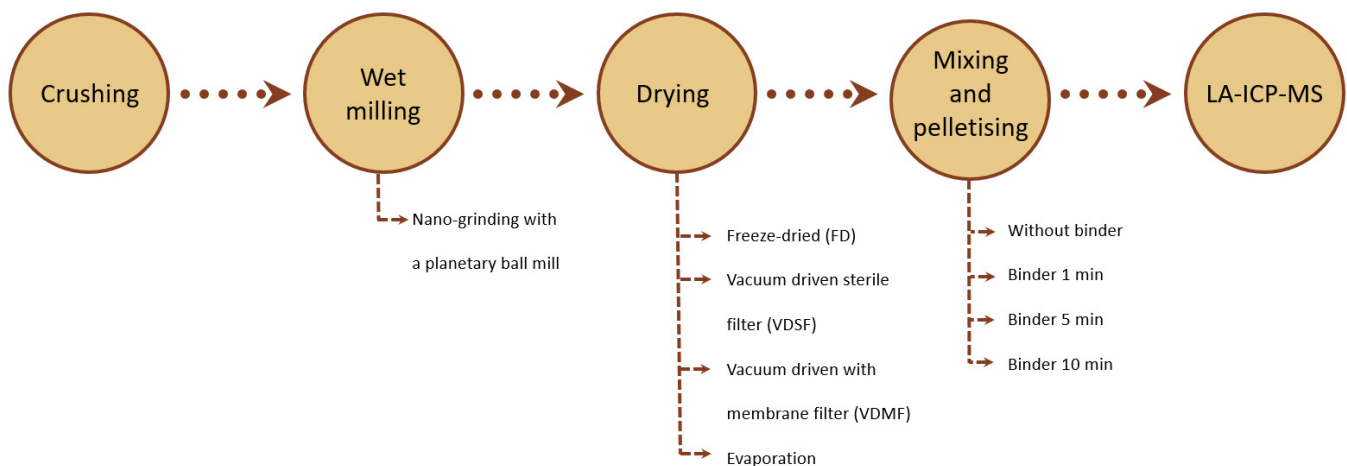
Figure 1. Flowchart of the pellet production and analysis process from whole-rock to analysis.

The application of the method was evaluated in two reference ores, one Ta ore and one W ore, selected for their critical metal contents. The reference ores were described in the materials section.

3.1. Wet Milling—Nano Grinding

In this study, all samples were nano-ground using a wet-milling procedure. The importance of achieving nano grain sizes to increase the chemical homogeneity of the resulting pellets has been demonstrated [2]. All powder ore samples were treated according to the nano-grinding protocol described by Garbe-Schönberg and Müller (2014) [2]. Samples were wet-milled in a high-power planetary ball mill (Fritsch Planetary Micro Mill Pulverisette 7, Laval Lab, Laval, QC, Canada) with two 45 mL ceramic vials and agate milling balls of 5 mL in diameter. For the nano-grinding, 2 gr of the sample were loaded with approximately 17 g of agate milling balls and 5 mL of high purity water. Agate milling balls were selected

due to the low contamination source, density, and hardness of agate, as suggested by Garbe-Schönberg and Müller, 2014 [2].

Each milling stage was performed using two vials. The milling process was carried out at consecutive time intervals of 10 cycles. Each cycle comprised intervals of 3 min milling followed by 3 min of cooling. The direction of the rotation was reversed after each milling interval. The total milling time was 30 min at 800 Hz.

After the milling process, the sample suspension was placed into another container. The milling balls and vials were carefully rinsed with high purity water from a pipette, followed by manual mixing and extraction of the second sample suspension. All sample suspension was mixed and accumulated in a recipient. The total amount of needed water or number of repetitions of this procedure was not set. This process was repeated until the collected fluid was clear, meaning that no sample material was present in the water solution. This methodology was suggested by Garbe-Schönberg and Müller, 2014 [2].

3.2. Drying

The third part relates to a drying stage where the water was removed from the sample suspension using four different techniques. The techniques used were freeze-drying (FD), vacuum-driven sterile filter (VDSF), vacuum-driven membrane filter (VDMF), and evaporation (E).

3.2.1. Freeze-Drying (FD)

After the wet milling and rinsing of the fluid, the sample suspension was stored in a freezer for a minimum of 24 h. After this time, a freeze-drying process of the sample suspension covered with a filter paper was applied. Freeze-drying constitutes dehydration by freezing the product at low pressure and removing the ice by sublimation. At the freezing stage, the material is cooled below the triple point of the water–ice–water vapor phase diagram, where sublimation occurs. The next step is lowering the pressure by a vacuum pump and heating to generate the sublimation and the consequential elimination of water. The water vapor is then reliquefied and solidified by a cold condenser chamber. During a second drying, the water molecules are removed. This stage is similar to the primary drying phase, but the temperature rises higher and the pressure lowers. After the freeze-drying process is complete, the vacuum is usually broken with inert N gas.
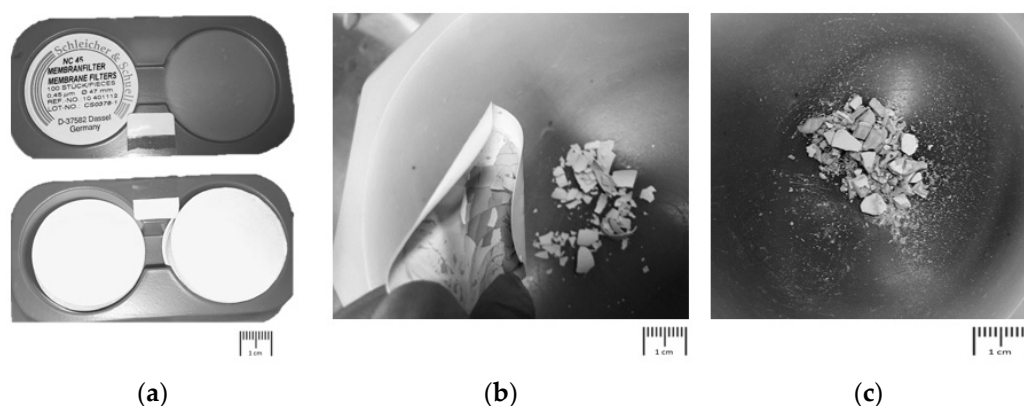
3.2.2. Vacuum-Driven Membrane Filter (VDMF)

Membrane filtration is a pressure-driven separation process that generates a mechanical and chemical separation using a membrane [20]. The filtration process aims to separate solid particles from the sample solution. The process was performed using a vacuum filtration with a Buchner funnel, a water aspirator assembly, and a membrane filter NC45 from Schleicher and Schell (45 μm) with a diameter of 47 mm. After the filtration process, the membrane with all solid particles was placed in the oven at 60 °C for 10 min. Once the particles were dried, they were separated from the filter, placed in an agate mortar, and pestled for manual homogenization. In Figure 2 shows the vacuum-driven membrane filter technique, the filter with dried particles and how to separate them from the filter.

3.2.3. Vacuum-Driven Sterile Filter (VDSF)

Like VDMF, a vacuum-driven sterile filtration process aims to separate solid particles from the sample suspension. The process was performed using a sterile disposable vacuum filter unit from MilliporeSigma. The sterile disposable vacuum filter had double lead thread with vacuum port with a volume of 50 mL. The membrane filter type was Steriflip-GV Filter Unit which has a pore size of 0.22 μm with a filtration area of 7 cm^2. After the filtration process, the membrane with all solid particles was placed in the oven at 60 °C for 15 min or until no more liquid remained. Once the particles were dried, they were separated from the filter, placed in an agate mortar, and pestled for manual homogenization. In Figure 3 it is

possible to observe the sterile disposable vacuum filter unit, the filter with dried particles, and how to separate them from the filter.

Figure 2. Vacuum-driven membrane filter. (**a**) Schleicher and Schell filter. (**b**) Dried particles in the filter. (**c**) Separation of the particles in the agate mortar.
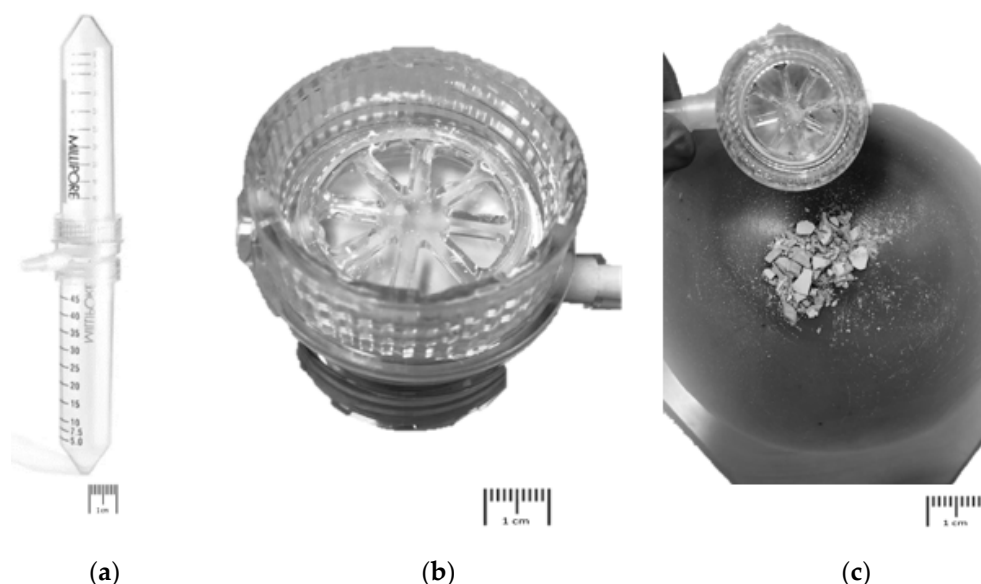
Figure 3. Vacuum-driven sterile filter technique. (**a**) Sterile disposable vacuum filter unit from MilliporeSigma. (**b**) Steriflip-GV Filter Unit as membrane filter with dried particles. (**c**) Separation of the rock particles from the filter and placed in an agate mortar.

3.2.4. Evaporation (E)

The dehydration technique was used to achieve the separation by evaporating the water using heat. The process involves heating the sample suspension in the oven at 60 °C for 30 min or until no more liquid remained. Once the particles were dried, they were placed in an agate mortar and pestled for manual homogenization.

3.3. Homogenization of the Nano-Powder, Binders, and Pressed Pellets

For homogenization, 200 mg of dried nano-powder was manually mixed and homogenized using an agate mortar and pestle for one minute in the case of pellets produced without binders. The use of an agate abrasion does not significantly affect the sample chemistry [10].

Some pellets were performed using cellulose as a binder. The binder selection was based on the work of Peters and Pettke (2017) [10]. The binders were microcrystalline cellulose powder of 20 μm from Aldrich (Buch, Switzerland MCC: $(C_6H_{10}O_5)$n; product

number: 310697). The sample nano-powder and binder were manually mixed and homogenized in an agate mortar and pestle in a mass ratio of sample to the binder of 4:1 (160 and 40 mg). Three homogenization times were used: 1 min, 5 min, and 10 min.

Pressed pellets were prepared using 200 mg of dry and homogenized nano-particle sample powders (with or without binder). The nano-powder samples were pressed into pellets using a standard pellet mold of stainless steel and a manual hydraulic press (equipment), applying a pressure of 10 tonnes for 10 min. The pellets were stored in a plastic container at room temperature with controlled humidity until chemical analysis.

3.4. LA-ICP-MS Analysis

Analyses were performed at the Microgeochemistry Laboratory at the Department of Earth Sciences, University Gothenburg, Gothenburg, Sweden. A NWR 213 ESI laser ablation system equipped with a Nd:YAG laser delivering a wavelength of 213 nm was used as a sampling system, connected to an Agilent 8800 ICP-QQQ mass spectrometer. Laser ablation was performed using circular spots of 100 μm diameter, laser pulse repetition rate of 5 Hz, laser fluence of about 3 $J \cdot cm^{-2}$, and ablation time of 40 s. An online pre-ablation of 2 s was performed before each analysis to eliminate any surface contamination. The sample cell was flushed with helium before the beginning of the experiment to expel air.

Carrier and auxiliary gas flow rates and plasma torch position were tuned for robust plasma conditions (low oxide formation, i.e., $^{232}Th^{16}O^{+}/^{232}Th < 0.004$, efficient ionization, i.e., $0.95 < {}^{238}U^{+}/^{232}Th^{+} < 1.05$) in a single quadrupole (no gas) mode by ablating a line (line width 50 μm, laser pulse repetition rate 10 Hz, laser fluence $\approx 5\ J \cdot cm^{-2}$) on the NIST SRM610, a standard glass enriched in most elements, at the beginning of each day of the experiment. Carrier gas flow rate ranged from 800 $mL \cdot min^{-1}$ to 900 $mL \cdot min^{-1}$ of high purity helium (Air Liquide, $\geq$99.999 vol%). High purity N_2 was added to the carrier gas before the plasma torch at a flow rate of 4 $mL \cdot min^{-1}$. Maximal sensitivity across the whole mass range (optimized for ^{89}Y while avoiding dramatic signal loss for ^7Li and ^{238}U) was achieved by tuning lenses and mass filter biases in a single quadrupole (no gas) mode. Ion lenses, acceleration potentials, and octopole RF were then re-optimized in MS/MS mode with an N_2O flow rate of 0.1178 $cm^3 \cdot min^{-1}$ (17% of the maximum flow rate on the fourth mass flow controller) to achieve maximum sensitivity on several oxides and dioxide productions. Energy discrimination (Q2 bias—Octopole bias) was kept at -20.0 V to ensure good transmission of the ions to the second quadrupole and the detector. A set of typical parameters is presented in Table 1. P/A factor calibration (co-calibration of the pulse and analog detectors for linearity across the signal range) was performed when non-linearity was observed during starting up and calibration.

High purity N_2O (Air Liquide, $\geq$99.999 vol%) was used as a reaction gas. N_2O is connected to the fourth mass flow controller on the Agilent 8800 (calibrated for N_2, 100% flow rate correspond to 0.693 $mL \cdot min^{-1}$ of N_2O). Before the experiment, the reaction gas was allowed to flow through the reaction cell overnight at a 15 % flow rate while the instrument was on standby to flush out gas impurities. High purity helium (Air Liquide, $\geq$99.999 vol%) is used as a buffer non-reactive collision gas in the reaction cell at a flow rate of 1 $mL \cdot min^{-1}$. Table 1 shows the typical analytical parameters.

The dwell time was set to 3 ms for all masses measured, and the results were converted in counts per second. The runs were set such that the analysis of reference materials was repeated after every ten sample analyses for drift correction.

The software GLITTER (4.4.2 sofware, developed by the ARC National Key Centre for Geochemical Evolution and Metallogeny of Continents (GEMOC) with input from CSIRO Exploration and Mining, California, USA) was used for data reduction, integrating the signal over the ablation time to get an average ion signal in counts per second. The background signal was integrated over about 10 s. Signal and background integration limits were chosen in an area of stable signal, but significant peaks (i.e., peaks likely due to inhomogeneities in the sample) were not excluded. Single signal spikes were filtered out using the filter function of the software. Counts per second were converted to concentration

in ppm using NIST 610 as external standards and the oxide values reported in Table 2 as internal standards.

Table 1. Typical analytical parameters used throughout this work. Ion lenses and acceleration voltages were optimized at the beginning of every day of the experiment (see text), so actual values may vary slightly from one experiment to another.

Laser					
He flow rate	$mL \cdot min^{-1}$	800	N_2 flow rate	$mL \cdot min^{-1}$	4
Fluence	$J \cdot cm^{-2}$	~3	Laser repetition rate	Hz	5
Spot size	μm	100	Pre-ablation	s	2
Ablation	s	40			
ICP-MS/MS					
Plasma					
RF power	W	1550	RF matching	V	1.7
Sampling depth	mm	4.0	Carrier gas (Ar)	$L \cdot min^{-1}$	1.22
Lenses					
Extract 1	V	−25.1	Extract 2	V	−250.0
Omega bias	V	−150	Omega lens	V	6.0
Q1 entrance	V	−12.0	Q1 exit	V	−3.0
Cell focus	V	−6.0	Cell entrance	V	−140
Cell exit	V	−70	Deflect	V	−0.4
Plate bias	V	−60			
Q1					
Mass gain		133	Mass offset		127
Axis gain		1.0005	Axis offset		0.07
Bias	V	−2.0	Prefilter bias	V	−10.0
Postfilter bias	V	−10.0			
Cell					
He flow rate	$mL \cdot min^{-1}$	1.0	N_2O flow rate	$mL \cdot min^{-1}$	0.1178
Octopole bias	V	−9.8	Octopole RF	V	190
KED	V	−20			
Detector					
Dwell time	s	0.0030	Integration time	s	40

Table 2. Oxide concentration (in weight percent) was used as an internal standard for the analyzed materials.

Material	**SiO$_2$**	**CaO**
Mittersil pellets	61.5 wt% [a]	6.28 wt% [a]
Penouta pellets	74.7 wt% [a]	0.1 wt% [a]
Oreas 24b pellet	66 wt% [b]	1.47 wt% [b]

[a] Whole-rock analysis through ICP-MS and ICP-AES. See Section 4. [b] Jochum et al., 2007 (GeoReM).

The obtained values are based on data normalized to SiO_2 as an internal standard due to the high content of this element.

3.5. ICP-MS and ICP-AES

Complementary to the LA-ICP-MS analysis, solution analysis was used to analyze the chemical composition of the ores. The standard bulk chemical analysis used fused bead and acid digestion of the samples, followed by inductively coupled plasma mass spectrometry (ICP-AES) and inductively coupled mass spectrometry (ICP-MS). The samples

were analyzed by acid digestion of fused bead by ICP-AES (major elements) and ICP-MS (trace elements) by ALS global. Refractory elements (e.g., Nb and Ta minerals) are challenging to digest, but fused samples were totally solubilized with sodium peroxide and then analyzed by ICP-MS.

4. Results and Discussion

The chemical homogeneity of the powder-pressed pellets produced by different drying methods is evaluated through LA-ICP-MS spot analysis of refractory ore elements. W concentrations of the Mittersil ore (W ore) and Ta, Nb, and Sn of the Penouta ore (Ta ore) are presented in Tables 3–6 and Figure 4.

Table 3. Summary of W concentrations (ppm) of the Mittersil ore pellets obtained by LA-ICP-MS spot analysis following pellet production using different drying techniques. The values are based on data normalized to SiO_2 as an internal standard. SD = standard deviation; rep = repeated analytical run.

Drying Method	Binder/ Homogenization Time	1	2	Spots 3	4	5	Mean	SD
				W (ppm)				
Freeze-dried (FD)	No binder	1882.83	2075.00	1936.49	2023.95	1941.42	1971.94	76.58
	1 min	2602.45	2784.00	2728.81	2593.84	2509.15	2643.65	110.93
	5 min	2225.36	1758.64	2044.25	1863.65	2218.22	2022.02	209.04
	10 min	2911.25	2431.81	2445.53	2741.83	2511.43	2608.37	210.14
	No binder (rep)	1756.82	1961.91	1997.41	1930.41	2045.89	1938.49	110.25
Vacuum filtration with membrane (VDMF)	No binder	2412.66	2314.15	2306.13	2398.19	2403.59	2366.94	52.19
	1 min	2080.00	2313.65	2230.31	2080.27	2223.54	2185.55	102.57
	5 min	2038.09	2047.90	2337.64	2314.56	2294.34	2206.51	150.09
	No binder (rep)	2236.21	2206.79	2118.70	2455.55	2209.05	2245.26	125.61
Vacuum-driven sterile filter (VDSF)	No binder	1715.14	1796.37	1778.92	1738.92	1854.99	1776.87	54.17
	1 min	1536.56	1587.82	1643.73	1664.81	1636.01	1613.79	51.56
	5 min	1576.91	1671.31	1666.77	1838.97	1768.51	1704.49	101.22
	10 min	1556.39	1604.23	1859.61	1691.56	1619.20	1666.20	118.49
Evaporation (E)	1 min	2354.49	2600.82	2336.43	2608.11	2648.31	2509.63	151.09
	5 min	2744.47	2639.57	2601.34	2656.24	3574.52	2843.23	412.16
	10 min	1930.42	2292.37	2090.10	1960.25	2023.62	2059.35	144.02
ICP-MS and ICP-AES reference value: 1967 ppm								

Table 4. Summary of the Ta concentrations (ppm) of the Penouta ore pellets obtained by LA-ICP-MS spot analysis following pellet production using different drying techniques. The values are based on data normalized to SiO_2 as an internal standard. SD = standard deviation; rep = repeated analytical run.

Drying Method	Binder/ Homogenization Time	1	2	3	4	5	Mean	SD
				Ta (ppm)				
Freeze-dried (FD)	No binder	71.42	57.66	78.97	66.36	81.33	71.15	9.61
	1 min	119.69	102.67	109.25	113.49	138.32	116.68	13.59
	5 min	89.54	116.58	91.60	101.95	129.82	105.90	17.13
	10 min	153.29	150.76	151.84	175.36	111.81	148.61	22.95
	No binder (rep)	153.29	67.50	60.67	66.95	70.07	83.70	39.06
Vacuum filtration with membrane (VDMF)	No binder	92.12	76.32	94.02	150.42	71.02	96.78	31.58
	1 min	74.59	81.42	73.37	139.57	84.87	90.76	27.70
	No binder (rep)	111.15	60.44	117.49	162.84	75.71	105.53	39.94

Table 4. *Cont.*

Drying Method	Binder/ Homogenization Time	1	2	3	4	5	Mean	SD
Vacuum driven sterile filter (VDSF)	1 min	55.64	63.95	59.46	67.54	63.67	62.05	4.59
	5 min	72.90	76.58	78.53	72.20	84.96	77.03	5.14
	10 min	57.78	57.20	62.50	55.58	59.45	58.50	2.63
Evaporation (E)	1 min	92.67	100.12	88.33	104.16	103.25	97.71	6.92
	5 min	58.03	71.24	64.30	114.24	71.55	75.87	22.16
	10 min	124.27	128.02	112.35	136.41	n.a.	125.26	9.99
ICP-MS&ICP-AES reference value: 97.3 ppm								

Table 5. Summary of the Nb concentrations (ppm) of the Penouta ore pellets obtained by LA-ICP-MS spot analysis following pellet production using different drying techniques. The values are based on data normalized to SiO_2 as an internal standard. SD = standard deviation; rep = repeated analytical run.

| Drying Method	Binder/Homogenization Time	1	2	3	4	5	Mean	SD
					Nb (ppm)			
Freeze-dried (FD)	No binder	68.68	50.91	67.04	53.90	73.11	62.73	9.74
	1 min	61.3	61.06	61.18	60.43	78.94	64.58	8.03
	5 min	70.85	73.21	61.01	70.23	82.63	71.59	7.73
	10 min	66.10	67.64	70.66	80.78	65.49	70.13	6.28
	No binder (rep)	66.10	55.37	54.40	53.76	54.41	56.81	5.23
Vacuum filtration with membrane (VDMF)	No binder	76.57	65.88	85.18	144.14	60.34	86.42	33.66
	1 min	51.67	79.35	51.67	70.85	68.49	64.41	12.31
	No binder (rep)	76.56	55.31	76.28	101.46	102.45	82.41	19.82
Vacuum-driven sterile filter (VDSF)	1 min	52.39	56.25	53.63	55.96	57.23	55.09	2.01
	5 min	55.31	63.58	61.29	58.99	62.44	60.32	3.28
	10 min	51.50	53.47	53.66	49.53	54.48	52.53	2.00
Evaporation (E)	1 min	59.82	62.24	56.78	65.95	65.33	62.02	3.83
	5 min	47.73	72.58	48.66	122.29	50.10	68.27	31.91
	10 min	69.86	54.03	53.17	76.65	n.a.	63.43	11.69
ICP-MS and ICP-AES reference value: 58.2 ppm								

Table 6. Summary of the Sn concentrations (ppm) of the Penouta ore pellets obtained by LA-ICP-MS spot analysis following pellet production using different drying techniques. The values are based on data normalized to SiO_2 as an internal standard. SD = standard deviation; rep = repeated analytical run.

Drying Method	Binder/Homogenization Time	1	2	Spots 3	4	5	Mean	SD
					Sn (ppm)			
Freeze-dried (FD)	No binder	249.72	228.83	281.32	201.36	230.65	238.38	29.55
	1 min	381.53	302.75	241.25	294.72	462.57	336.56	86.43
	5 min	281.07	259.13	261.26	280.35	301.51	276.66	17.28
	10 min	313.93	341.3	354.06	313.79	321.76	328.97	17.96
	No binder (rep)	313.93	187.44	191.62	181.32	171.83	209.23	59.00
Vacuum filtration with membrane (VDMF)	No binder	300.02	309.22	331.09	303.13	348.71	318.43	20.83
	1 min	316.95	244.6	342.00	265.28	346.66	303.10	45.98
	No binder (rep)	395.73	333.69	250.95	376.06	398.91	351.07	61.71

Table 6. *Cont.*

Drying Method	Binder/Homogenization Time	1	2	Spots 3	4	5	Mean	SD
Vacuum-driven sterile filter (VDSF)	1 min	245.32	214.06	232.28	224.51	226.07	228.45	11.48
	5 min	234.13	267.84	243.00	231.19	247.9	244.81	14.52
	10 min	216.79	213.04	219.14	214.22	221.92	217.02	3.61
Evaporation (E)	1 min	344.41	327.58	303.39	273.69	301.86	310.19	27.02
	5 min	235.63	285.65	231.31	272.32	222.68	249.52	27.70
	10 min	337.08	278.13	284.06	259.87	n.a.	289.79	33.17

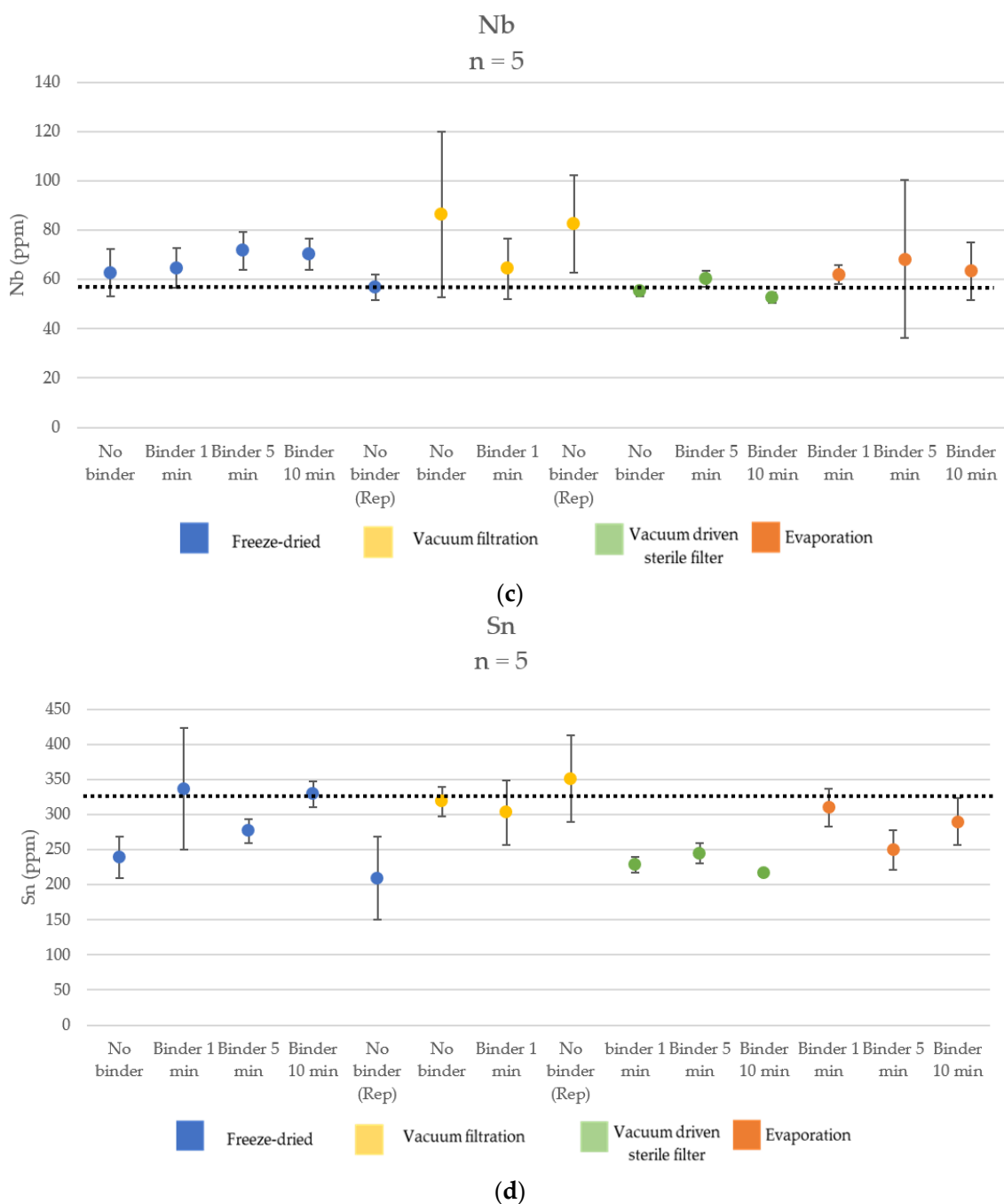ICP-MS and ICP-AES reference value: 329 ppm

(**a**)

(**b**)

Figure 4. *Cont.*

(c)

(d)
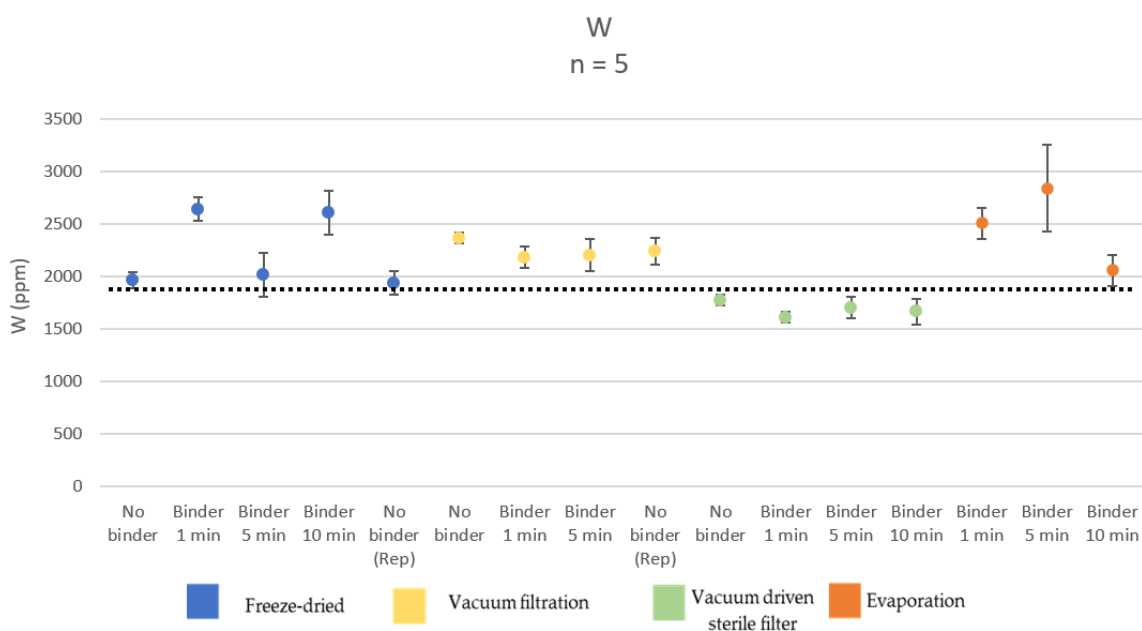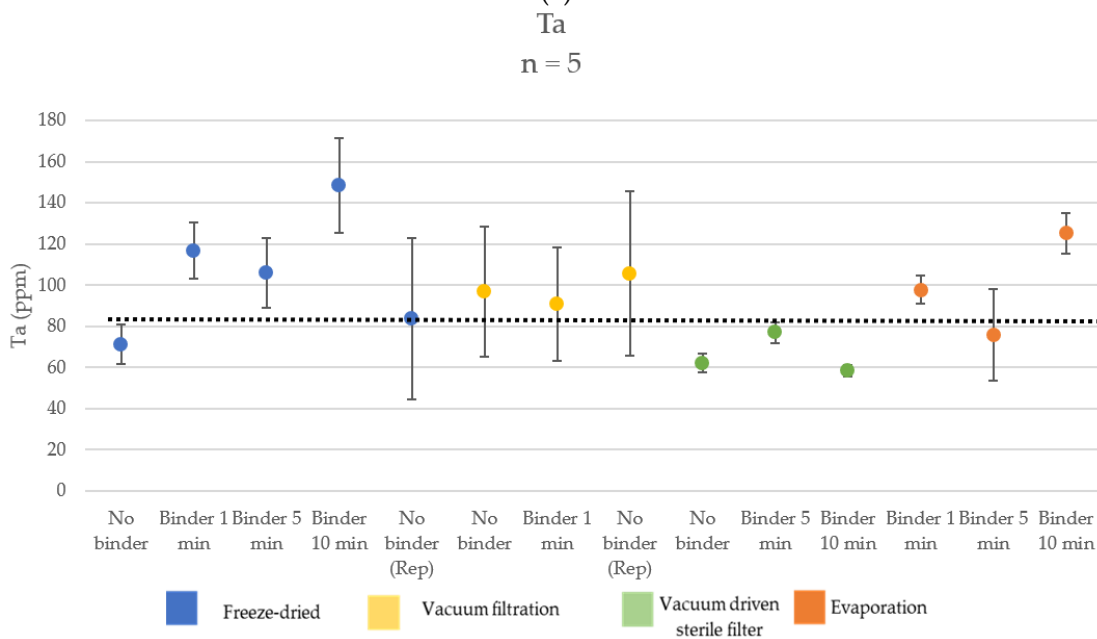
Figure 4. Summary of the element content of the Penouta and Mittersill ore pellets after LA-ICP-MS using different drying techniques in ppm. (**a**) Data for tungsten (W) in Mittersil ore, (**b**) data for tantalum (Ta) in Penouta ore, (**c**) data for niobium (Nb) in Penouta ore, and (**d**) data for tin (Sn) in Penouta ore.

4.1. Chemical Binders

The samples produced without a binder from powder dried by vacuum-driven sterile filter and evaporation techniques resulted in fractured and incoherent pellets (Figure 5). For the other drying techniques, the usage of binders resulted in mechanically stable and robust pellets, in line with previous observations that binders increase the cohesion and compatibility of pressed pellets [6].

(a)   **(b)**
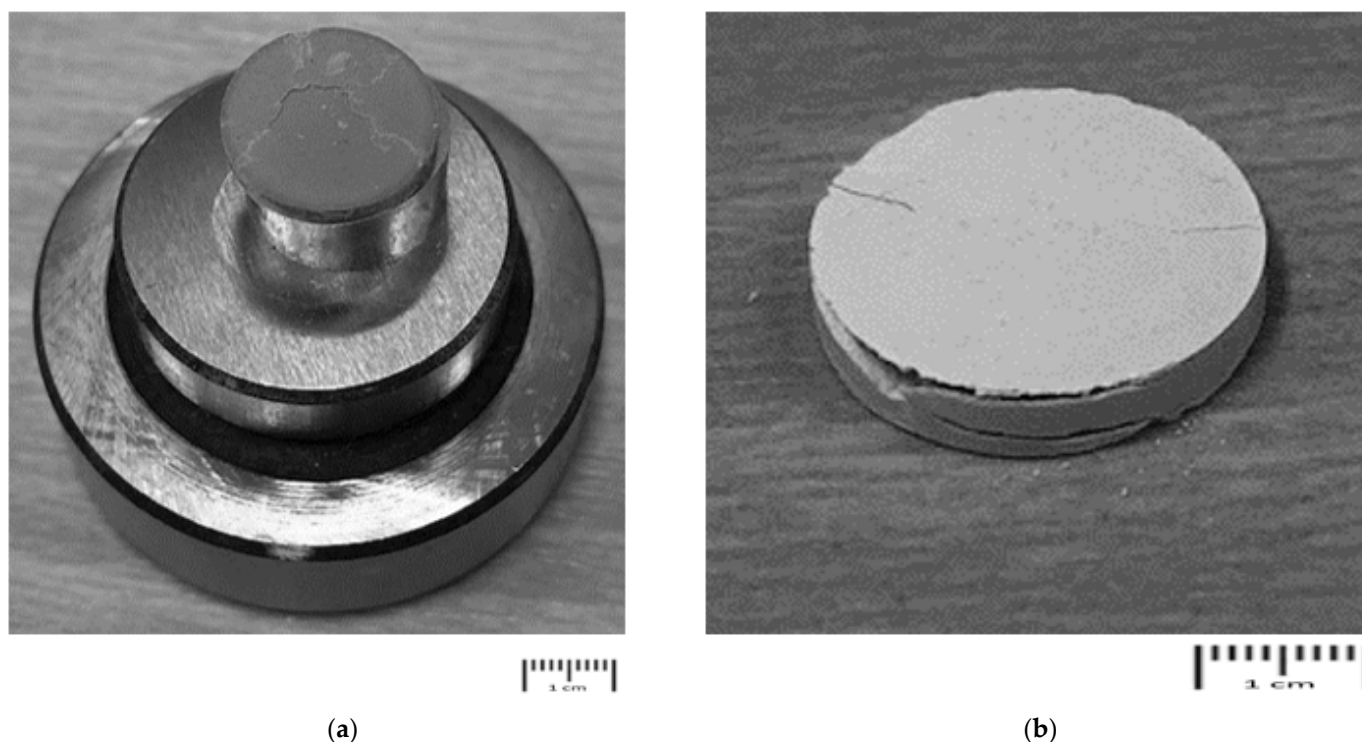
Figure 5. Fractured and incoherent pellets produced without binders. (**a**) Mittersill ore pellet produced using evaporation drying technique. (**b**) Penouta ore pellet produced using evaporation drying technique.

Apart from helping the mechanical properties, the use of binders in the pellets did not result in differences in the element concentrations compared to samples produced without binders (Tables 2–5), indicating that binders allow high repeatability and accuracy of measurements [10]. The diluting effect of the chemical binder that caused a lower concentration of some elements in powder-pressed pellets noted in the study of Liu et al., 2013 [6] was not detected during our analysis. The utilization of binders may thus allow drying techniques, such as evaporation or filtering, that are faster, easier, and economically viable to apply than freeze-drying in pellet production chains. Furthermore, the homogenization time between the ore powder and the binder did not influence the results of the values. The pellets with binder homogenization times of 1 min, 5 min, and 10 min show low variability values in almost all analytical runs (Figure 4a). It was also observed that the use of cellulose binders in a mass ratio of sample to the binder of 4:1 enhances the compatibility and mechanically stability of the pellets in addition to improving measurement repeatability and accuracy [2,5–7].

4.2. Reproducibility of Repeated Analyses

In addition, the FD pellets without binder and VFMF pellets without binder were subject to repeated analytical runs. The precision and accuracy of the method were evaluated for each analyzed element (W, Ta, Sn, and Nb) using the calculated mean value and standard deviation of five spot measurements on each pellet (Figure 4, and Tables 3–6). The mean values obtained by repeated analyses of W concentrations in Mittersill pellets using the FD technique were similar, at 1972 ± 77 ppm and 1938 ± 110 ppm. The same applies for the FD Penouta pellet, the Sn values vary between 238 ± 30 and 209 ± 59 ppm, and the Nb values between 63 ± 9.7 ppm and 57 ± 5.2 ppm, whereas Ta displays a high standard deviation on the repeated analytical run (83 ± 39 ppm) due to a Ta peak in the first spot. Apart from this peak, the concentration values demonstrate the accuracy and repeatability of the FD method.

In the supplementary material are presented Tables S1–S4, where the values of the powder-pressed pellets produced by the different drying methods with the difference of normalization are shown; in these tables, the values are based on data normalized to CaO as an internal standard. As it is possible to observe, differences are presented, and the values and accuracy show marked similarities. This means that regardless of the internal standard used, the accuracy of the method is the same.

The accuracy of LA-ICP-MS based on the repeated measurement of the standards has shown outstanding results for Nb and Sn, where the relative standard deviation is below 10%. The LA-ICP-MS and bulk chemical analysis (ICP-MS and ICP-AES) accuracy for the shown cases is better than 10%. This value is a comparatively small error concerning sampling errors and imperfect homogenization during grinding.

4.3. Chemical Heterogeneity

The error margins and the standard deviation values of each analysis are functions of the samples' homogeneity and the analytical method's reproducibility. The LA-ICP-MS method was proven reproducible and provided information on the sample homogeneity in the individual signal of each spot analysis. In these signals, peaks and heterogeneities were detected in several spots, corresponding to uneven distribution of rock or mineral fragments rich or poor in refractory metals in the sample. The signal variations thus evidence chemical heterogeneity, possibly accompanied by grain size heterogeneities. Heterogeneities are probably causing enhanced standard deviations and analytical error margins (Tables 3–6). Optimized grinding procedures for the refractory ore metal minerals are likely to decrease errors and standard deviations by increasing homogeneity in individual pellets and among the pellets of the same sample. Considering that the variances in the values might be generated by inclusions of some particles that have been difficult to grind and be reduced in nano-sized grains, a better grinding of the tantalum particles is needed. Enhanced homogeneity could be achieved by using equipment more efficiently or by adopting longer grinding times.

4.4. Ore Metal Loss by VDSF

Another trend occurring throughout the dataset is that all element concentrations from VDSF were lower than the concentrations from the rest of the techniques in all cases (Figure 4); between 10% and 18% lower for W, from 21% to 40% lower for Ta, and between 12 and 22% for Sn. These low concentrations represent mineral particles lost from the sample during drying, rendering VDSF unreliable. However, the standard deviations from VDSF are also low, suggesting that this drying method results in a homogenous pellet of the particles that do pass the filter stage. VDSF may thus still be recommended for finer grinded grain sizes. The loss of particles due to incomplete rinsing after each grinding session is disregarded as a possible source of lower concentrations in the LA-ICP-MS spot analyses than the reference values in our methodological procedure since we followed the protocol established by Garbe-Schönberg and Müller, 2014 [2], to ensure that no particles remained on the milling balls after grinding.

4.5. Evaluation of the Drying Techniques

The offset numbers to the reference value are measured from the absolute mean concentrations without regarding the error margins outlined in Figure 2. The offset in element concentrations obtained by LA-ICP-MS spot analysis compared to the reference value for the freeze-dried pellets is a maximum of 34% for W, 53% for Ta, 23% for Nb, and 36% for Sn. The use of binders did not affect the precision of the data, and the production of cohesive pellets was possible without binders. However, the technique is less economically viable than other drying methods evaluated in this study since it is time-consuming and requires expensive equipment. In contrast, the VDMF technique is simple, without specialized equipment. The offsets in element concentrations obtained by LA-ICP-MS compared to the ICP-MS and ICP-AES values are lower than 20% for W, 8% for

Ta, and 8% for Sn. These offset values are generally lower than for the other techniques. The offset up to 48% for Nb represents the highest Nb offsets, but the high analytical errors of LA-ICP-MS data for Nb nevertheless overlap the reference value (Figure 4c). The evaporation technique offers results similar to the VDMF but with higher offsets for W and Ta and higher offsets from the reference values for most analyses. As a simple technique without the need for any specific equipment, evaporation drying can be helpful in combination with a binder.

4.6. Application of PP-LA-ICP-MS in Mineral Test Work

Mineral processing test work commonly involves geochemical analysis of complex elements, e.g., refractory elements (e.g., Nb, Ta, Cr) and volatile components (e.g., As, Cd, Sn) and precious elements that are hard to dissolve (e.g., Au) in concentrations ranging from parts per billion to weight percent. XRF analysis of pressed pellets is a handy tool for this purpose since it allows rapid and affordable sample preparation and analysis directly at the test lab. However, at low concentrations (<100–1000 ppm depending on element and matrix), heterogeneities and calibration may be a challenge, and the precision and accuracy of XRF may not be fit for purpose. In this case, analysis typically has to be performed using more sensitive techniques, e.g., INAA or analysis of dissolved (± fusion) samples by ICP-MS or ICP-AES in specialized laboratories. These analyses are time-consuming, with a turnaround of several weeks that significantly slows down the iterative processes of mineral test work. LA-ICP-MS is a standard technology at universities and research organizations, and setting up a collaboration with a local partner can significantly reduce the turnaround time. The production of pressed nano-particulate pellets with micro cellulose as the binder is very similar to producing high-quality pressed pellets for XRF analysis. With a modest investment in a high-energy laboratory ball mill combined with a press and dye set, the pellet production can be performed in-house at the test lab. Most LA-ICP-MS labs can analyze hundreds of spot analyses per day, and typically have spare capacity, and thus it is possible to decrease the turnaround from weeks to days.

5. Conclusions

Methods for the production of pressed-powder pellets were developed and evaluated by analyzing the chemical composition of the refractory metals W, Ta, Nb, and Sn in ores from two different sites using LA-ICP-MS. These elements are recovered primarily within error compared to a reference value obtained by solution ICP-MS and ICP-AES, suggesting LA-ICP-MS spot analysis is a simple alternative for expensive and time-consuming solution techniques. Our tested methods yielded pressed-powder pellets with suitable cohesion, homogeneity, and mechanical stability for LA-ICP-MS analysis. The pellets contained nano-particles produced through wet milling and drying by four different techniques; freeze-drying, VDSF, VDMF, and evaporation drying. The results demonstrated that freeze-drying, VDMF, and evaporation drying gave element concentrations within the margin of error of the reference value, whereas material was lost during VDSF. Pelletization was performed both with and without a binder. Repeated analysis within individual pellets enabled the evaluation of accuracies and reproducibility. The errors and standard deviation values may be reduced further through optimized grinding procedures. Furthermore, it is shown that the use of cellulose binders in a mass ratio of sample to binder of 4:1 increases the compatibility and mechanical stability of the pellets. It was also observed that the homogenization time does not affect the measured element concentrations.

standard. SD = Standard deviation, rep = repeated analytical run. Table S3. Summary of the Nb concentrations (ppm) of the Penouta ore pellets obtained by LA-ICP-MS spot analysis following pellet production using different drying techniques. The values are based on data normalized to CaO as an internal standard. SD = Standard deviation, rep = repeated analytical run. Table S4. Summary of the Sn concentrations (ppm) of the Penouta ore pellets obtained by LA-ICP-MS spot analysis following pellet production using different drying techniques. The values are based on data normalized to CaO as an internal standard. SD = Standard deviation, rep = repeated analytical run.

References

1. Pinto, F.G.; Junior, R.E.; Saint'Pierre, T.D. Sample preparation for determination of rare earth elements in geological samples by ICP-MS: A critical review. *Anal. Lett.* **2012**, *45*, 1537–1556. [CrossRef]
2. Garbe-Schönberg, D.; Müller, S. Nano-particulate pressed powder tablets for LA-ICP-MS. *J. Anal. At. Spectrom.* **2014**, *29*, 990–1000. [CrossRef]
3. Yu, Z.; Robinson, P.; McGoldrick, P. An evaluation of methods for the chemical decomposition of geological materials for trace element determination using ICP-MS. *Geostand. Newsl.* **2001**, *25*, 199–217. [CrossRef]
4. Robinson, P.; Townsend, A.T.; Yu, Z.; Münker, C. Determination of Scandium, Yttrium and Rare Earth Elements in Rocks by High Resolution Inductively Coupled Plasma-Mass Spectrometry. *Geostand. Newsl.* **1999**, *23*, 31–46. [CrossRef]
5. Ito, K.; Hasebe, N.; Sumita, R.; Arai, S.; Yamamoto, M.; Kashiwaya, K.; Ganzawa, Y. LA-ICP-MS analysis of pressed powder pellets to luminescence geochronology. *Chem. Geol.* **2009**, *262*, 131–137. [CrossRef]
6. Liu, Y.; Hu, Z.; Li, M.; Gao, S. Applications of LA-ICP-MS in the elemental analyses of geological samples. *Chin. Sci. Bull.* **2013**, *58*, 3863–3878. [CrossRef]
7. Miliszkiewicz, N.; Walas, S.; Tobiasz, A. Current approaches to calibration of LA-ICP-MS analysis. *J. Anal. At. Spectrom.* **2015**, *30*, 327–338. [CrossRef]
8. Gray, A.L. Solid sample introduction by laser ablation for inductively coupled plasma source mass spectrometry. *Analyst* **1985**, *110*, 551–556. [CrossRef]
9. Holá, M.; Otruba, V.; Kanický, V. Influence of binders on infrared laser ablation of powdered tungsten carbide pressed pellets in comparison with sintered tungsten carbide hardmetals studied by inductively coupled plasma atomic emission spectrometry. *Spectrochim. Acta Part B At. Spectrosc.* **2006**, *61*, 515–524. [CrossRef]
10. Peters, D.; Pettke, T. Evaluation of major to ultra trace element bulk rock chemical analysis of nanoparticulate pressed powder pellets by LA-ICP-MS. *Geostand. Geoanalytical Res.* **2017**, *41*, 5–28. [CrossRef]
11. Guldris Leon, L.; Hogmalm, K.J.; Bengtsson, M. Understanding Mineral Liberation during Crushing Using Grade-by-Size Analysis—A Case Study of the Penuota Sn-Ta Mineralization, Spain. *Minerals* **2020**, *10*, 164. [CrossRef]
12. Mukherjee, P.K.; Khanna, P.P.; Saini, N.K. Rapid Determination of Trace and Ultra Trace Level Elements in Diverse Silicate Rocks in Pressed Powder Pellet Targets by LA-ICP-MS using a Matrix-Independent Protocol. *Geostand. Geoanalytical Res.* **2014**, *38*, 363–379. [CrossRef]
13. Alfonso, P.; Hamid, S.A.; García-Vallès, M.; Llorens, T.; Moro, F.L.; Tomasa, O.; Polonio, F.G. Textural and mineral-chemistry constraints on columbite-group minerals in the Penouta deposit: Evidence from magmatic and fluid-related processes. *Mineral. Mag.* **2018**, *82*, S199–S222. [CrossRef]
14. Anticoi, H.; Guasch, E.; Hamid, S.A.; Oliva, J.; Alfonso, P.; Garcia-Valles, M.; Peña-Pitarch, E. Breakage function for HPGR: Mineral and mechanical characterization of tantalum and tungsten ores. *Minerals* **2018**, *8*, 170. [CrossRef]
15. González, T.L.; Polonio, F.G.; Moro, F.J.L.; Fernández, A.F.; Contreras, J.L.S.; Benito, M.C.M. Tin-tantalum-niobium mineralization in the Penouta deposit (NW Spain): Textural features and mineral chemistry to unravel the genesis and evolution of cassiterite and columbite group minerals in a peraluminous system. *Ore Geol. Rev.* **2017**, *81*, 79–95. [CrossRef]
16. Rosario, J.V.N. Caracterización Del Comportamiento Cinético en Molienda de Varias Menas de Tántalo y Wolframio. Ph.D. Thesis, Universidad de Oviedo, Oviedo, Spain, 2021.
17. López, F.A.; García-Díaz, I.; Rodríguez Largo, O.; Polonio, F.G.; Llorens, T. Recovery and purification of tin from tailings from the Penouta Sn–Ta–Nb deposit. *Minerals* **2018**, *8*, 20. [CrossRef]

18. Ahmad Hamid, S.; Alfonso, P.; Oliva, J.; Anticoi, H.; Guasch, E.; Hoffmann Sampaio, C.; Garcia-Vallès, M.; Escobet, T. Modeling the liberation of comminuted scheelite using mineralogical properties. *Minerals* **2019**, *9*, 536. [CrossRef]
19. Thalhammer, O.; Stumpfl, E.; Jahoda, R. The Mittersill scheelite deposit, Austria. *Econ. Geol.* **1989**, *84*, 1153–1171. [CrossRef]
20. Benjamin, M.M.; Lawler, D.F. *Water Quality Engineering: Physical/Chemical Treatment Processes*; John Wiley & Sons: Hoboken, NJ, USA, 2013.